Aeolian Research 23 (2016) 11–20

Contents lists available at ScienceDirect

Aeolian Research

journal homepage: www.elsevier.com/locate/aeolia

Evolving flux of Asian dust in the North Pacific Ocean since the late Oligocene

Wenfang Zhang, Jun Chen, Junfeng Ji, Gaojun Li *

MOE Key Laboratory of Surficial Geochemistry, Department of Earth Sciences, Nanjing University, 163 Xianlindadao, Nanjing 210023, China

ARTICLE INFO

Article history:
Received 5 June 2016
Revised 10 September 2016
Accepted 12 September 2016

Keywords:
Deserts
Tibetan Plateau
Loess
Atmospheric dust
Climate change

ABSTRACT

The aeolian deposits in the North Pacific Ocean (NPO) serve as important archives for the surface processes in the arid Asian interior. Aeolian flux, which is usually based on the 'operationally defined aeolian dust' (ODED) extracted from the pelagic sediments, is a widely used paleo-proxy that reflects aridity of the source regions. However, such reconstruction of aeolian flux is subject to large uncertainty associated with the age model due to the low sedimentation rate and lack of calcareous nannofossil of the pelagic sediments. Precipitation of authigenic minerals and contribution of volcanic ash also complicate interpretation of the reconstructed ODED flux. This work extracts ODED from the sediments recovered at Ocean Drilling Program (ODP) site 1208 on the Shatsky Rise in NPO. The high sedimentation rate at ODP site 1208 enables a high-resolution age model. The resulting ODED flux, which shows a progressive increasing trend over the past 25 Ma, is very different from the previous reconstructions. The study indicates that authigenic phillipsite contribute a significant portion to the sediment of 25–18 Ma, but the relative contribution of Asian dust to the ODED is roughly constant (60–80%) over the past 18 Ma. Thus, the progressive increasing trend of ODED flux at the ODP site 1208 is not contributed by authigenic phillipsite and volcanic ash but reflect the increasing flux of Asian dust. We propose that the increasing flux of Asian dust in NPO reflects the progressive aridification of Asian interior in response to global cooling and/or regional mountain building.

© 2016 Elsevier B.V. All rights reserved.

1. Introduction

Asia interior is the second largest center of dust emission in the world (Engelbrecht and Derbyshire, 2010). The aeolian deposits of Asian dust in the Chinese loess, the pelagic sediments of NPO, and the Greenland ice cores serve as important archives for the late Cenozoic climate changes (Biscaye et al., 1997; Guo et al., 2002; Rea et al., 1998). Aeolian flux is one of the mostly used proxies that is believed to reflect the aridity of Asian interior (e.g., Sun and An, 2005). The best records for the long-term changes in flux of Asian dust is in the central NPO, where the pelagic sediment can extend back to the early Cenozoic Era (Pettke et al., 2002).

The pelagic sediment in NPO is mainly composed of the mineral dust from the Asian interior and volcanic ash from the circum-Pacific volcanoes with precipitates of authigenic minerals, hydrothermal products, and biogenic organic carbon, opal and carbonate (Nakai et al., 1993; Ziegler et al., 2007). A chemical procedure, which involves sequential leaching by weak acid, reductive and oxidative reactants, and alkaline solution, has been employed to remove the carbonate minerals, amorphous Fe-Mn hydroxides, organic matter, and biogenic opal in the pelagic sediment (Rea and Janecek, 1981). The leaching residue, which is mainly detrital silicates, is regarded as 'operationally defined aeolian dust' (ODED) (Olivarez et al., 1991; Rea and Janecek, 1981). Flux of the ODED (F_{ODED}, g/cm^2/ka) is then can be calculated from the faction of ODED in the bulk sample (f_{ODED}, g/g) given that dry bulk density (D, g/cm^3) and deposition rate (R, cm/ka) of the sediments were known (Rea and Janecek, 1981):

$$F_{ODED} = f_{ODED} \times D \times R \quad (1)$$

The reconstructed fluxes of ODED in NPO show a dramatic increase since 3–4 Ma (Janecek, 1985; Janecek and Rea, 1983; Rea et al., 1998). However, the detailed evolutions of F_{ODED} are very different among different sites. For example, the F_{ODED} reconstructed from ODP 885/886 sites shows a pronounced increase at ~8 Ma, and then a decreasing trend until the second increasing step at ~3.6 Ma (Rea et al., 1998). The first increasing step of F_{ODED} has not been registered in the site LL44-GPC3 and DSDP site 576 (Janecek, 1985; Janecek and Rea, 1983). However, the first increasing step of F_{ODED} recorded in ODP site 885/886 has been frequently

* Corresponding author.
E-mail address: ligaojun@nju.edu.cn (G. Li).

http://dx.doi.org/10.1016/j.aeolia.2016.09.004
1875-9637/© 2016 Elsevier B.V. All rights reserved.

referred to reflect the increasing aridity of Asian interior regardless the inconsistence with the other records (Guo et al., 2004; Pettke et al., 2000; Sun and An, 2002; Zheng et al., 2004).

It is unlikely that the flux of Asian dust evolves differently among the different sites in the NPO because Asian dust has been largely dispersed after long-range transportation. Geochemical signature for the contribution of Asian dust in the pelagic sediments has been detected all cross the NPO (Nakai et al., 1993; Olivarez et al., 1991; Pettke et al., 2000, 2002; Seo et al., 2014; Serno et al., 2014; Stancin et al., 2006; Weber et al., 1996). The limited changes in position of the depositional sites associated with seafloor spreading also cannot explain the inconsistent record of F_{ODED} among the different sites (Snoeckx et al., 1992). One of the major errors in calculating the F_{ODED} in Eq. (1) is sourced from the sedimentation rate (R). The pelagic sediments in NPO are characterized by low deposition rate of several meters per million years (Janecek and Rea, 1983; Rea et al., 1993, 1998). The slow deposition rate and the early recovery (before 1990s) of the ODP and DSDP cores prevent high-resolution magnetic reversal stratigraphy (Janecek and Rea, 1983; Rea et al., 1993, 1998). The pelagic sediments in the deep NPO are mostly deposited below the carbonate compensation depth, and thus are subject to extensive dissolution of carbonate. Therefore, the widely used biotic stratigraphy based on calcareous nannofossil is generally inapplicable (Janecek and Rea, 1983; Rea et al., 1993, 1998).

Contribution of volcanic ash and authigenic minerals may also influence the reconstructed F_{ODED} (Weber et al., 1996; Ziegler et al., 2007). The sites that are close to the margin of NPO receive much higher input of volcanic ash from the circum-Pacific volcanoes than the sites in the central NPO (Nakai et al., 1993). Authigenic mineral has been found to contribute a significant portion to the silicate component in the sediments of eastern NPO (Hyeong et al., 2005; Rea et al., 1993; Ziegler and Murray, 2007; Ziegler et al., 2007). Contribution of authigenic mineral, volcanic ash, and Asian dust to the ODED can be resolved by trace element composition and the radiogenic Nd and Sr isotopic ratios (Jiang et al., 2013; Nakai et al., 1993; Weber et al., 1996; Ziegler et al., 2007). Authigenic mineral precipitated from seawater is characterized by high concentration of total REE, LREE depletion, and negative Ce anomaly (Piepgras and Jacobsen, 1992). The volcanic ash, which is in basaltic and andesitic composition, is characterized by low $^{87}Sr/^{86}Sr$ ratio, high ε_{Nd} value, and high contents of mafic elements such as Sc, Ni, Co, Cr (Defant et al., 1990; Nakai et al., 1993; Olivarez et al., 1991; Weber et al., 1996). The Asian dust show similar composition to the upper continental crust with high $^{87}Sr/^{86}Sr$ ratio, low ε_{Nd} value, and high contents of lithophile elements such as Th, Rb, and U (Nakai et al., 1993; Olivarez et al., 1991; Taylor and McLennan, 1985; Weber et al., 1996).

This study reconstructs aeolian flux in NPO based on the sediments recovered from ODP site 1208 on the Shatsky Rise. The age model of the sediments from ODP site 1208 has been well constrained by magnetic reversal stratigraphy and biotic stratigraphy benefited from the high sedimentation rate and the well preserved biogenic carbonate and opal (Shipboard Scientific Party, 2002). Contribution of Asian dust, volcanic ash, and authigenic minerals in the ODED will be resolved by the trace element compositions and the radiogenic Nd and Sr isotopic ratios.

2. Samples and method

2.1. Materials

Bulk sediments of the past 25 Ma were collected from ODP site 1208 and core LL44-GPC3 in the NPO. Core-top samples of late Pleistocene age were also collected from fourteen DSDP/ODP sites in the northwest Pacific Ocean (Fig. 1). In addition, the <5 μm silicate fractions of three loess samples and twenty-six surface sand samples from the ten major deserts in Asian interior (Supplementary Fig. S1) were split from the same samples that were used to constrain the Nd and Sr isotopic composition of Asian dust in our previous studies (Chen et al., 2007; Li et al., 2009).

ODP site 1208 (36°7.6301′N, 158°12.0952′E) is located on the center of the central high of the Shatsky Rise at a water depth of 3346 m (Shipboard Scientific Party, 2002). Coring at site 1208 has recovered an expanded, apparently complete upper Miocene to Holocene section of nannofossil ooze and nannofossil clay between 0 and 251.6 mbsf (meter below sea floor), below which lies almost 60 m of a less expanded lower and middle Miocene section (Shipboard Scientific Party, 2002). A high-resolution age model has been established by biochronologic and magnetic stratigraphy applied onboard to the research vessel (Shipboard Scientific Party, 2002) (Fig. 2a). Two sets of samples have been collected from the ODP 1208 core. A low-resolution sample set that covers the past 25 Ma was collected at proximately equal time interval at resolution of about 3 samples per million years. A high-resolution sample set spanning 250 kyr of time at approximately 2.75 Ma ago was collected at resolution of about 2.5 k.y. per sample. The chronologic

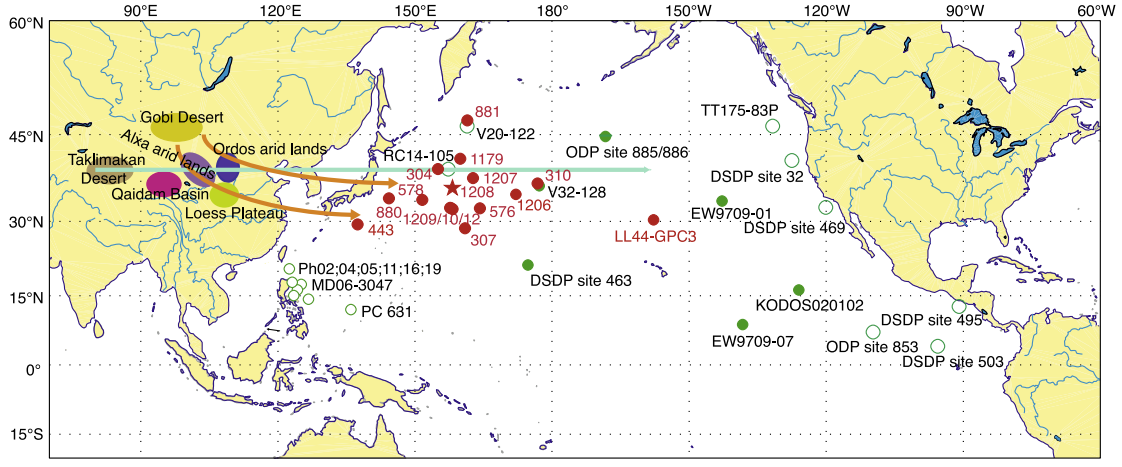

Fig. 1. Map showing the locations of ODP Site 1208 and other sites in North Pacific Ocean. Sites labeled with red-filled circles are the sites studied in this work. Sites labeled with open green and green-filled circles are those with published Nd-Sr isotopic data in circum-Pacific and north central Pacific regions, respectively. The shaded areas in the Asian Interior are the potential source regions of Asian dust. Yellow and green arrows indicate transportation of Gobi and Taklimakan dust by the East Asian winter monsoon and westerly wind, respectively. (For interpretation of the references to color in this figure legend, the reader is referred to the web version of this article.)

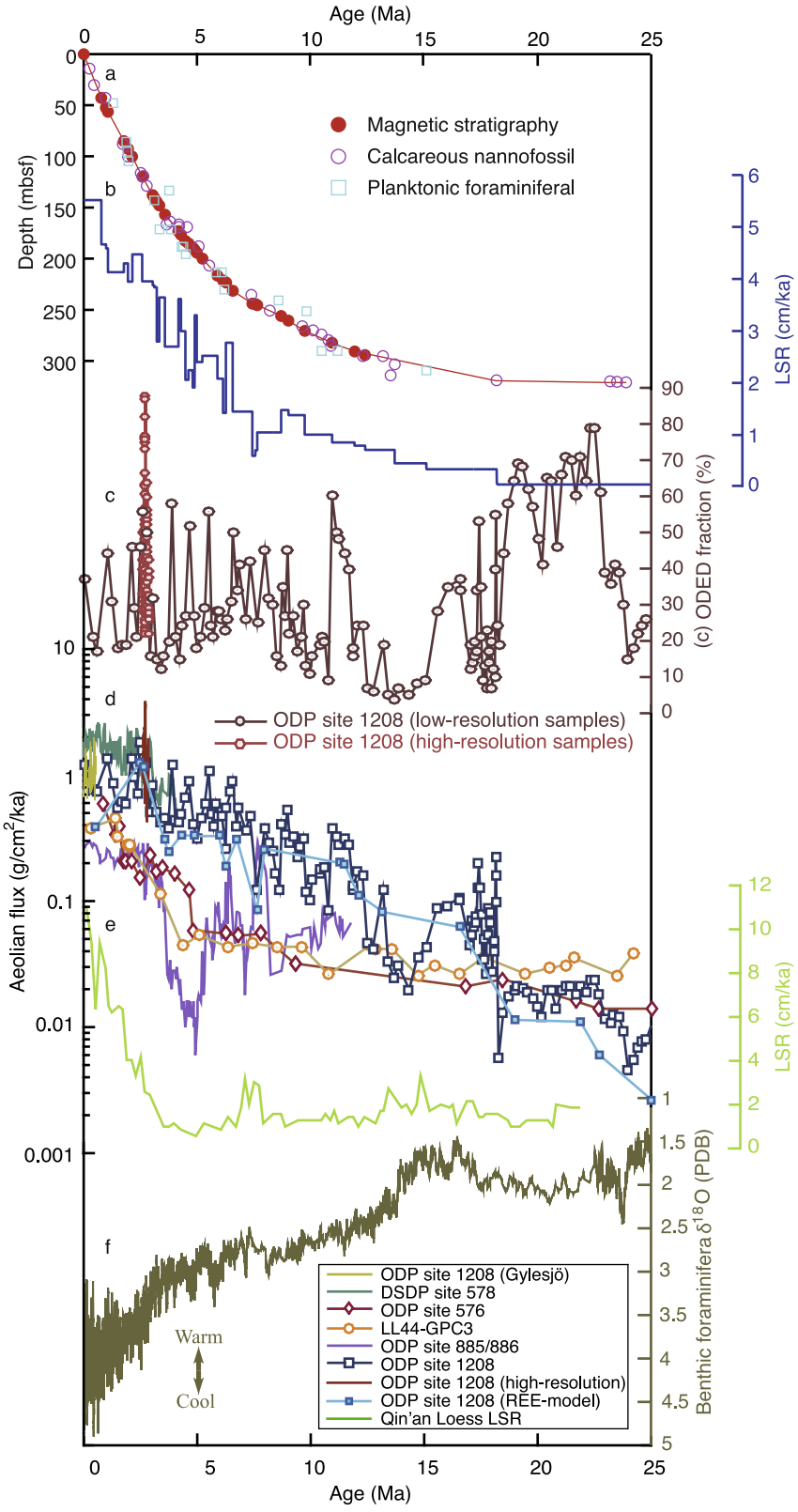

Fig. 2. Time series of the ODED flux compared with other records. (a)–(d), age model, linear sedimentation rate (LSR), ODED fraction, and the ODED flux at ODP site 1208. Data could be found in Supplementary Table S1. The age model is derived from calcareous nannofossil and planktonic foraminifera bio-stratigraphy and magnetic stratigraphy from the initial reports (Shipboard Scientific Party, 2002) using the geomagnetic polarity timescale of Cande and Kent (1995). Fitting of the age-depth curve is only based on magnetic stratigraphy when data are available. The late Pleistocene aeolian fluxes of ODP Site 1208 from Gylesjö (2005) are presented in (d) for comparison. Also compared in (d) are ODED fluxes at other sites in the North Pacific Ocean (Rea et al. (1998), Janecek and Rea (1983), Janecek (1985)), the pure Asian aeolian dust flux (REE-model) calculated by the relative proportion of Asian dust in the ODED fraction. (e) and (f) are the linear sedimentation rate (LSR) of Qin'an Loess in China (Guo et al., 2002) and the oxygen isotopic composition of benthic foraminifera that reflects global ice volume and/or temperature (Zachos et al., 2001), respectively.

framework of the high-resolution samples has been developed by correlating the $\delta^{18}O$ record of benthic foraminifera to the LR04 $\delta^{18}O$ stack (Venti and Billups, 2012).

The large-diameter piston core LL44-GPC3 was recovered at 30°19.9′N, 157°49.9′W, 5705 m water depth. The sediments and stratigraphy have been described in detail by Janecek and Rea (1983). About 21 samples that cover the past 25 Ma are collected from the LL44-GPC3 core at a resolution of 0.8 samples per million years on average.

The ODED component of the pelagic sediments was extracted using the method of Rea and Janecek (1981). Briefly, about 4 g of the dry bulk sample was dissolved in diluted acetic acid (0.5 mol/L) overnight to remove the carbonate component. Then, the organic matter is removed by 5% H_2O_2. After repeated cleaning by deionized water, the amorphous Fe and Mn oxides and hydroxides in the non-carbonate component were removed in a sodium dithionite-sodium citrate solution buffered with sodium carbonate at a temperature of 80 °C. The suspended solution was then passed through a 500-mesh (28 μm) sieve. Microscopic observation indicates the particles larger than 28 μm are mainly diatoms and radiolarians (Supplementary Fig. S2) because the aeolian dust from Asian interior and circum-Pacific volcano generally has grain size less than 8 μm (Hovan et al., 1991; Janecek, 1985; Janecek and Rea, 1983, 1985; Rea et al., 1998). Ideally, a smaller sieve can make a better separation of diatoms but sieving with smaller sieves is physically difficult. We thus dissolve the remaining opal in the <28 μm portion in a 0.4 N sodium carbonate solution for 30 min in a boiling water bath. The residue after opal removal is mainly composed of detrital silicate minerals (Supplementary Fig. S3), which is defined as ODED (Olivarez et al., 1991).

2.2. Trace element composition

The extracted ODED of the Pacific sediments and the <5 μm silicate fractions of Asian deserts and Chinese loess samples were completely digested with lithium metaborate/lithium tetraborate mixture in a furnace at 1025 °C. The resulting melt is then cooled and dissolved in an acid mixture containing nitric, hydrochloric and hydrofluoric acids. The trace element concentration in the solution was then analyzed by an inductively coupled plasma mass spectrometry (ICP-MS, Agilent 7700x) in ALS Chemex Co Ltd, Guangzhou, China. Analytical uncertainties were less than 5%.

2.3. Nd and Sr isotopes

Approximately 50 mg of the extracted ODED samples were dissolved in a mixture of HNO_3 and HF for 36 h in a tightly closed teflon vials at 120 °C. The Sr and Nd elements in the resultant solution were then purified using cation exchange techniques (Zhang et al., 2015). Briefly, Sr is separated using Sr-Spec resin, and Nd is separated by Ln-Spec resin following an enrichment of REEs by Tru-Spec resin (Aciego et al., 2009). About 150 ng Sr and 100 ng Nd were determined using a Neptune Plus Multi-Collector Inductively Coupled Plasma Mass Spectrometer (MC-ICP-MS) at the MOE Key Laboratory of Surficial Geochemistry, Department of Earth Sciences, Nanjing University. The instrumental mass bias for Sr and Nd isotopes was corrected by normalizing the $^{86}Sr/^{88}Sr$ ratio to 0.1194 and the $^{146}Nd/^{144}Nd$ ratio to 0.7219, respectively. The analytical blank was <1 ng for Sr and <60 pg for Nd. Strontium standard SRM987 and neodymium standard JMCNd$_2O_3$ were periodically measured to check the precision and accuracy of isotopic analyses with a mean $^{87}Sr/^{86}Sr$ ratio of 0.710239 ± 42 (2 σ external standard deviation, n = 10) and mean $^{143}Nd/^{144}Nd$ ratio of 0.512099 ± 15 (2 σ external standard deviation, n = 15), respectively. The standard material, BCR-2 is used to verify the chemical procedure. Measurements of ten replicates yielded a mean $^{87}Sr/^{86}Sr$ value of 0.705015 ± 20 (2 σ external standard deviation, n = 10) and a mean $^{143}Nd/^{144}Nd$ value of 0.512630 ± 15 (2 σ external standard deviation, n = 10). For convenience, the $^{143}Nd/^{144}Nd$ ratios are reported in the epsilon notation (ε_{Nd}), where $\varepsilon_{Nd} = (^{143}Nd/^{144}Nd_{sample}/^{143}Nd/^{144}Nd_{CHUR} - 1) \times 10000$, CHUR stands for Chondritic Uniform Reservoir with $^{143}Nd/^{144}Nd$ ratio of 0.512638 (Jacobsen and Wasserburg, 1980).

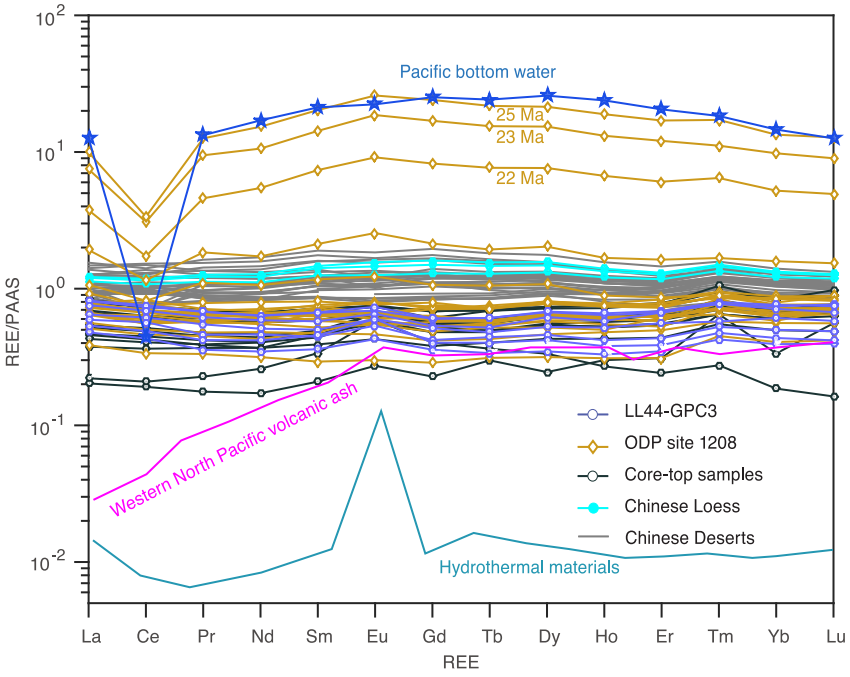

Fig. 3. PAAS-normalized REE patterns. Data could be found in Supplementary Tables S2 and S3. Data of volcanic ash in western North Pacific Ocean, hydrothermal materials, and the Pacific bottom water are from Bailey (1993), Severmann et al. (2004), and Ziegler et al. (2007), respectively.

3. Results

The reconstructed flux of ODED from ODP site 1208 shows a progressive increasing trend of two-order of magnitude since the late Oligocene (Fig. 2d). The increasing ODED flux is mainly contributed by the increasing sedimentation rate of the same two-order of magnitude because the fraction of ODED in the sediment of ODP 1208 core show no long-term increasing trend (Fig. 2b and c).

The samples of the past 18 Ma from ODP 1208 core show flat PAAS (Post-Archean Australian Shale) normalized REE patterns that are similar to the <5 μm silicate fractions of Asian deserts and Chinese loess (Fig. 3). However, the samples of 18–25 Ma are characterized by depletions of LREE and strong negative Ce anomaly (Fig. 3). These samples are also characterized by high REE concentration. In the triangular plot of La-Th-Sc, most of the samples from ODP 1208 core, northwest Pacific core-top sediments, and core LL44-GPC3 locate in the mixing line defined by the upper continental crust and the ocean crust (Fig. 4). Exceptions are samples of 18–25 Ma in ODP 1208 core due to the high La concentration. Positive Eu anomaly is also detected in some of the core-top samples and sediment in core ODP 1208 and LL44-GPC3. Those samples are also characterized by lower total REE concentration and enrichment of HREEs (Fig. 4).

The Nd and Sr isotopic compositions of the ODED in core ODP 1208 and LL44-GPC3 show similar trends of evolution (Fig. 5). The ε_{Nd} values decrease by about 1.5 unit and $^{87}Sr/^{86}Sr$ ratios decrease by 0.006 from ~18 Ma to ~3 Ma. After ~3 Ma, the trend of the Nd-Sr isotopic evolution reverses to the values of early Miocene. Along this long-term evolution is large short-term variation in ODP 1208 core (Fig. 5). Such short-term variation is absent in the core LL44-GPC3. The samples from LL44-GPC3 core and fourteen DSDP/ODP sites distribute along the mixing line defined by the volcanic ash and the dust from Taklimakan Desert in the binary plot between $^{87}Sr/^{86}Sr$ ratio and ε_{Nd} value. However, the samples from ODP 1208 core show much scatter pattern along this mixing line (Fig. 6).

4. Discussion

The high REE content, LREE depletion, and negative Ce anomaly of the samples of 25–18 Ma at ODP 1208 core indicate contribution of authigenic mineral. The X-ray Diffraction and Scanning Electronic Microscopy (SEM) analysis from the ODED samples at ODP 1208 show that the authigenic mineral is phillipsite (Supplementary Figs. S4 and S5). The phillipsite mineral in the 25 Ma-aged sample is relatively pure (the elemental compositions (EDS results) are illustrated in Supplementary Fig. S5), but invisible in the 2.64 Ma-aged sample (Supplementary Fig. S3). The phillipsite minerals were also reported to contribute a significant portion to the silicate components at eastern NPO sediments (Hyeong et al., 2005; Ziegler et al., 2007). The formation of phillipsite indicated that the sediments have likely experienced a significant diagenetic history (Ziegler et al., 2007). Phillipsite is suggested as one of the main carriers of REE in pelagic sediments (Piper and Wandless, 1992) and the REE pattern records the importance of chemical uptake from seawater or porewater during its formation (Piepgras and Jacobsen, 1992). Thus, the survived phillipsite after the chemical treatment by Rea and Janecek (1981) poses a significant challenge for the interpretation of paleoclimate proxies (Ziegler et al., 2007; Olivarez et al., 1991). The positive Eu anomaly and enrichment of HREE in the samples indicate contribution of volcanic ash. Those samples with flat PAAS normalized REE pattern indicate dominance of Asian dust. Mixing between volcanic ash and Asian dust can explain the trace element composition for most of the samples in the ODP 1208 core excepting for the samples of 25–18 Ma due to the input of authigenic phillipsite (Fig. 7).

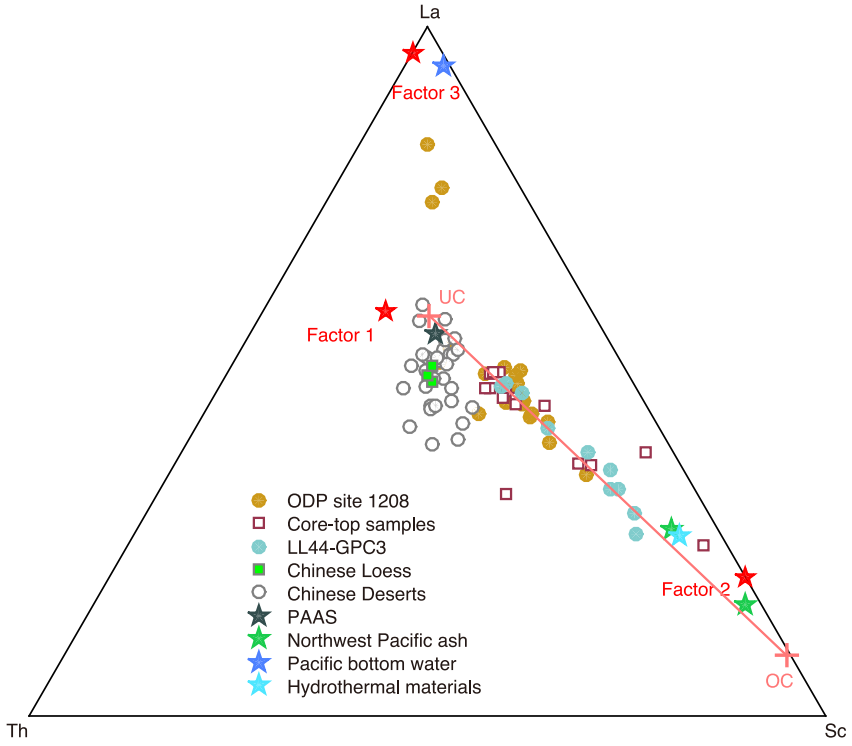

Fig. 4. La-Th-Sc ternary diagram. Data can be found in Supplementary Tables S2 and S3. The composition of PAAS, upper continental crust (UCC) and oceanic crust (OC) are from Taylor and McLennan (1985). Composition of northwest Pacific ash, Pacific bottom water, and hydrothermal materials are from Bailey, (1993), Ziegler et al. (2007), and Severmann et al. (2004), respectively. Also shown are the end-members generated by the factor analysis (Supplementary Table S4).

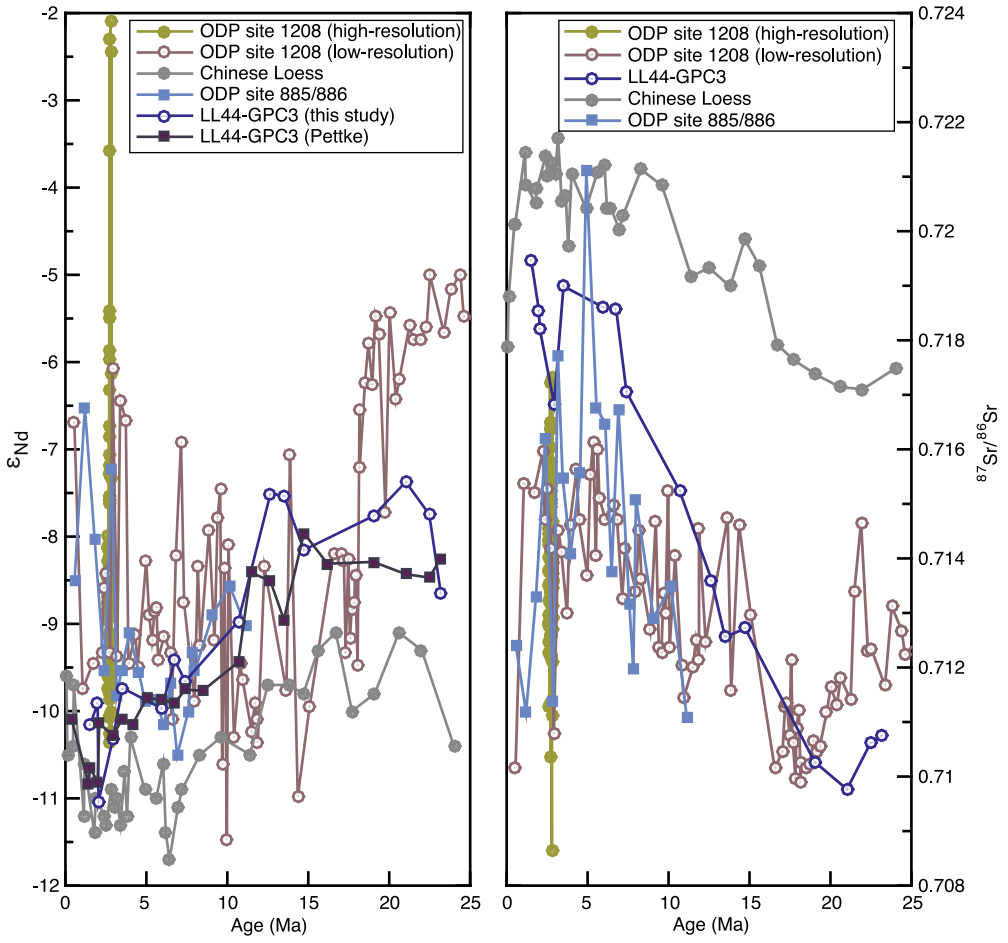

Fig. 5. Nd (a) and Sr (b) isotopic evolution of the ODED components archived in north Pacific sediments. Data for the ODP site 1208 and LL44-GPC3 can be found in Supplementary Tables S5–S7. The Nd and Sr isotopic compositions in sites 885/886 are from Pettke et al. (2000) and the previously analyzed ε_{Nd} values of core LL44-GPC3 are from Pettke et al. (2002). Also shown are Nd and Sr isotopic compositions of the 28–45 μm silicate fractions of Chinese loess (Chen and Li, 2013).

The relative contributions authigenic phillipsite in the ODED extracted from the sediment of ODP 1208 core can be calculated by a Q-model factor analysis and constrained least squares (CLS) multiple linear regression applied to the selected trace element compositions, following the methods described in Pisias et al. (2013). The Q-model factor analysis is performed using the selected trace elements, La, Ce, Sm, Eu, Sc and Th, to determine the composition of potential end-member sources in the Pacific sediments (Olivarez et al., 1991; Pisias et al., 2013; Weber et al., 1996). The subsequent CLS could then be used to quantify the contents of these end-members in each sample (Olivarez et al., 1991; Pisias et al., 2013; Weber et al., 1996). The results confirm that authigenic phillipsite dominates the sediment of late Oligocene and early Miocene in ODP core 1208 (Fig. 7). However, the contribution of authigenic phillipsite decrease dramatically to ~10% since 15 Ma. The CLS analysis also shows a roughly increasing contribution of Asian dust and relatively decreasing contribution of volcanic ash to the ODED since 15 Ma with the relative contribution of Asian dust ranges from 60% to ~80% (Fig. 7). Thus, the increasing ODED flux over the last 25 Ma is not contributed by increasing contribution of authigenic phillipsite or volcanic ash. We noticed that some researches, e.g. Ziegler et al. (2007), use the combined major and trace elements for the Q-model factor analysis and CLS multiple linear regression model. The joint of major elements would benefit the identification and discrimination for the potential end-members, although the trace element composition has already showed great success in discriminating the potential end-members (Olivarez et al., 1991; Weber et al., 1996). It is regret that the major element concentrations of the ODED samples were not measured in this study. This is because the original samples have already used up to extract the ODED fractions and the ODED fractions also have already been used up for the isotope and trace elements analysis.

One factor that complicates resolving the source of the ODED is the scatter pattern along the binary mixing line between volcanic ash and Asian dust in the cross-plot of Nd and Sr isotopic compositions (Fig. 6). We argue that the scatter pattern is caused by the heterogeneities of volcanic ash and Asian dust that is recorded by samples of high sedimentation. Volcanic ash of circum-Pacific volcano show large variation in Nd and Sr isotopic compositions with the $^{87}Sr/^{86}Sr$ ratio and the ε_{Nd} value ranging from 0.702610 to 0.706102 and from −6.7 to 10.4, respectively (Defant et al., 1990; Kepezhinskas et al., 1997; McCulloch and Perfit, 1981; Svensson et al., 2000; Woodhead, 1989) (Fig. 6). The Nd and Sr contents of the volcanic ash may also have large variations and thus influence the shape of the mixing lines between the volcanic end-member and Asian dust end-members.

It should be noticed that the Asian dust end-members are based on the <5 μm grain size fraction of silicate, while the particle size of ODED samples in this study is <28 μm (See samples and method). A bias might be produced by the comparison of ODED and Asian dust end-members with different particle sizes. Nevertheless, the <5 μm grain size fraction of Asian dust end-members was chosen because this fraction might be taken as representative of both

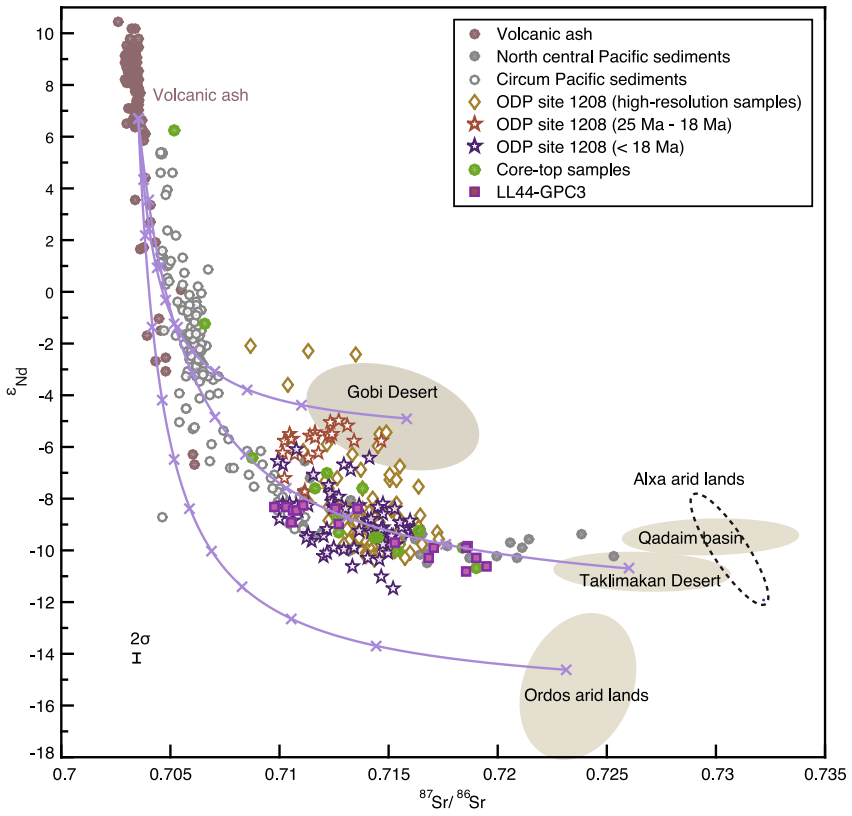

Fig. 6. Cross plot between the $^{87}Sr/^{86}Sr$ ratios and ε_{Nd} values of the ODED in Pacific sediments. Data can be found in Supplementary Table S5–S8. The Nd and Sr isotopic ratios of volcanic ash follow the published values (Defant et al., 1990; Kepezhinskas et al., 1997; McCulloch and Perfit, 1981; Svensson et al., 2000; Woodhead, 1989). The ranges of Nd and Sr isotopic compositions of the potential dust sources in Asia Interior (Taklimakan desert, Gobi desert, Ordos arid lands, Alxa arid lands, and the Qaidam basins) are based on previous studies (Bory et al., 2003; Chen et al., 2007; Li et al., 2011; Zhao et al., 2014, 2015). Also shown are the published Nd and Sr isotopic compositions of the sediments from North central Pacific and Circum Pacific (Jiang et al., 2013; Nakai et al., 1993; Pettke et al., 2000; Seo et al., 2014; Xu et al., 2015). The curve show mixing lines in 10% steps between the volcanic ash and Asian dust sources with Nd and Sr element concentrations of the potential sources based on the <5 μm silicate fractions of Chinese deserts (Supplementary Table S3 and Zhao et al. (2014)).

regionally and long-range transported Asian dust (Ferrat et al., 2011). It was also found that the REE patterns for the <4 and 4–16 μm fractions were nearly identical (Ferrat et al., 2011). The grain size analysis shows that the median diameter of the selected high-resolution ODED samples is less than 8 μm (Supplementary Fig. S6), consistent with previous studies (e.g. Hovan et al., 1991; Janecek, 1985). Thus, we argue that the bias caused by the particle size is very limited.

It has also been argued that the artifacts in REE concentrations introduced by the re-adsorption likely result in the artifacts of Nd isotopic compositions for the ODED sediments (Piper and Wandless, 1992; Sholkovitz, 1989). The procedure of Rea and Janecek (1981) is a sequential leaching, with the first step being acidic and the buffered dithionite one being alkaline. This leaching technique might affect the REE patterns through selective re-adsorption. As suggested by Sholkovitz (1989), the chemical leaching techniques have major artifacts associated with non-selectivity and re-adsorption of trace metals. However, Piper and Wandless (1992) preclude significant re-adsorption of the REE by the insoluble phases during the leaching procedure and the re-adsorption of REE would be insignificant. Later study concluded that leaching of various oceanic sediments at different solid/liquid ratios did not reveal REE re-adsorption by sediment (Dubinin and Strekopytov, 2001). Thus, we propose that the leaching procedure may not have influenced on the REE composition and Nd isotopes in this study. Nevertheless, a precaution action has been applied. We use large solution/sample ratio and rapid centrifuge separation during the reductive cleaning to minimize possible re-adsorption.

The scatter pattern along the binary mixing line between volcanic ash and Asian dust in the cross-plot of Nd and Sr isotopic composition may largely reflect changing source of Asian dust in response to the adjustment of atmospheric circulation. Although Taklimakan desert has been suggested as the major source region, signature of Gobi dust and the dust from Ordos arid lands has also been detected in the long-range transported dust such as those observed in the ice cores and snow deposits in Greenland (Biscaye et al., 1997; Bory et al., 2003; Zhao et al., 2015). A shift of dust source from Taklimakan Desert to the Gobi Desert will increase the ε_{Nd} value and decrease the $^{87}Sr/^{86}Sr$ ratio of Asian dust, while the dust from the Ordos arid lands is characterized by low ε_{Nd} value and high $^{87}Sr/^{86}Sr$ ratio (Fig. 6).

The combination of source variation and changing composition of volcanic ash may explain the large scatter pattern of the Nd and Sr isotopic compositions observed in the sediments with high deposition rate (e.g., the ODP 1208 core). However, for the sediments with low deposition rate (e.g., LL44-GPC3 core), these variations, presumably being in short-term, may have been largely averaged. Thus, a nice binary correlation can be observed between the average volcanic ash and average Asian dust for the sediments with low deposition rate (Fig. 6). Nevertheless, the long-term Nd and Sr isotopic evolution of the ODED in ODP 1208 core do replicates previous sediments cores but with much larger short-term fluctuations (Fig. 5). The long-term trend might be caused by decreasing relative contribution of volcanic ash in response to the increasing flux of Asian dust. The short-term fluctuations may have recorded the changing

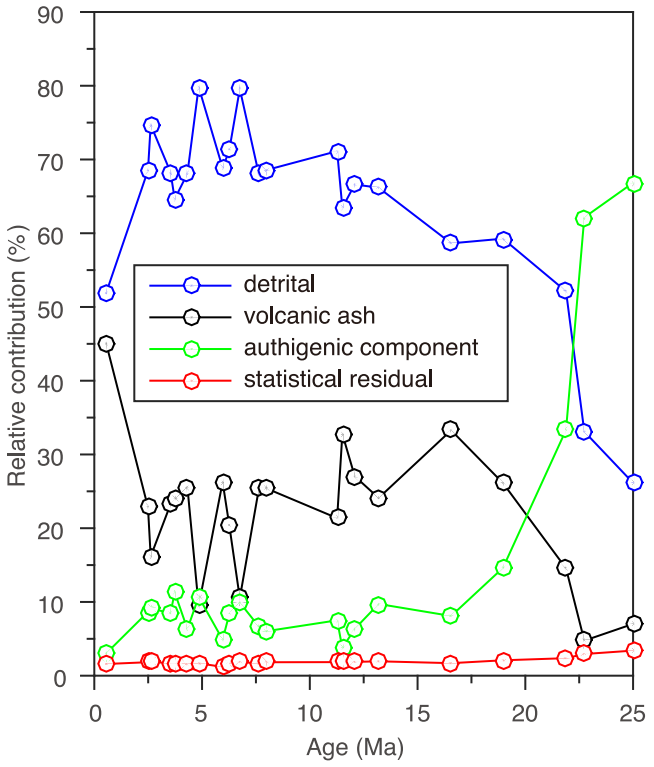

Fig. 7. Relative contributions of end-members for the ODED in ODP site 1208 generated by the Q-model factor analysis and CLS that applied to the trace element compositions.

composition of Asian dust and/or volcanic ash, which may otherwise have been averaged at the sites with low sedimentation rate.

Another complication for interpreting the ODED flux is the possible contribution of drift sediments as suggested by the initial report of ODP 1208 core according to the high sedimentation rate (Shipboard Scientific Party, 2002). However, the reconstructed late Quaternary ODED flux at the ODP 1208 site, averaged at 1.1 g/cm^2/kyr (Gylesjö, 2005), is not exceptionally high compared to the adjacent sites and is consistent with the exponential decreasing trend along the eastward transportation of Asian dust (Fig. 8). The grain size analysis of high-resolution ODED samples during Plio-Pleistocene transition at site 1208 show median diameter of less than 8 μm (Fig. S6), which is consists with the other records of aeolian dust in north pacific sediments (e.g. Hovan et al., 1991; Janecek, 1985). Thus, together with other evidences, we propose that the silicate fractions at ODP Site 1208 are derived principally from aeolian input rather than drift deposits.

The progressive increasing flux of Asian dust as recorded in the ODP site 1208 may reflect the aridity of Asian interior in response to global and/or regional climate change. The aridity-evolving pattern is corroborated by the significant increase of Asian dust in north central Pacific Ocean as shown by increasing detrital contribution and quartz content since the early Miocene (Leinen and Heath, 1981; Ziegler et al., 2007). Global cooling would enhance the aridification of Asian interior by reducing the water vapor in atmosphere (Dupont-Nivet et al., 2007; Miao et al., 2016). The aridification of Asian interior may also response to the uplift of Tibetan Plateau, which inhibit the penetration of moisture-bearing air mass from the oceans. The progressive and stepwise growth of Tibetan Plateau (Tapponnier et al., 2001; Wang et al., 2012) may be responsible to the development of desertification in Asian interior (An et al., 2001). However, the timing and history of Tibetan uplift is still under hot debates (Molnar and Tapponnier, 1975; Wang et al., 2011; Yin, 2010), which probably coevolve with global cooling trend according to the uplift driven cooling hypothesis of Cenozoic climate (Raymo and Ruddiman, 1992). Thus, resolving the role of global climate cooling and regional tectonic uplift on

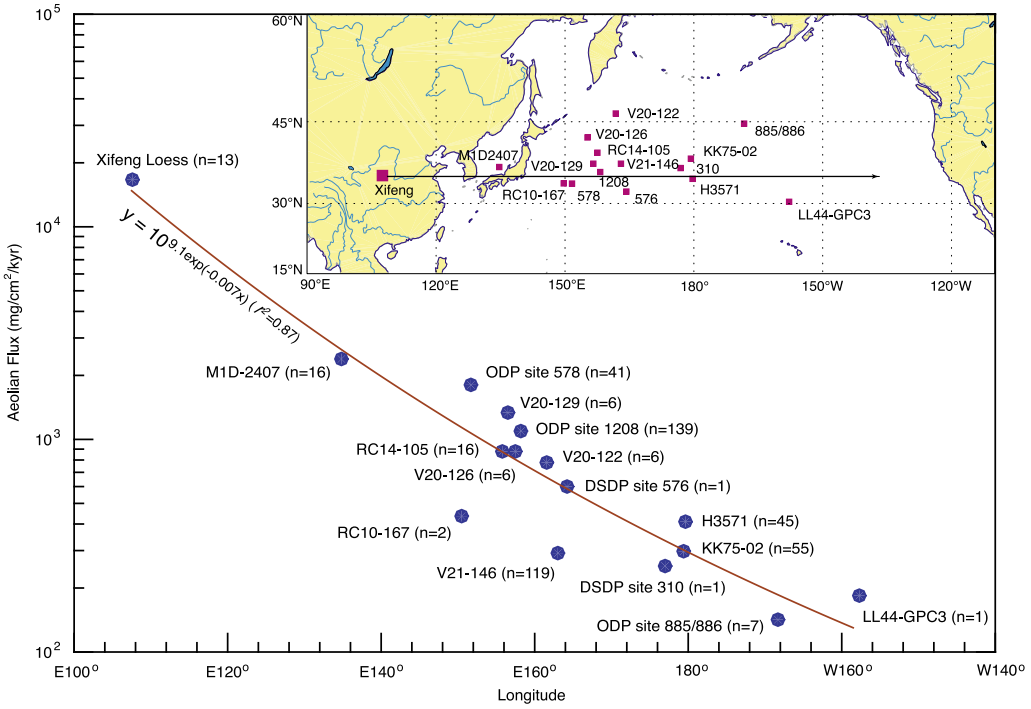

Fig. 8. Late-Quaternary (past 500 ka) aeolian flux in Pacific cores and Chinese Loess Plateau vs. distance (indexed by longitude) relative to the Asian interior. The inserted diagram shows the locations of the sites. Data sources: DSDP sites 310 and Core LL44-GPC3 (Rea and Janecek, 1982); Core V21-146 (Hovan et al., 1991); Core KK75-02 (Janecek and Rea, 1985); ODP sites 885/886 (Rea et al., 1998); Core V20-122, Core V20-126, Core RC14-105, Core RC10-167 and Core V20-129 (Rea and Leinen, 1988); DSDP sites 578 and 576 (Janecek, 1985); Core H3571 (Kawahata et al., 2000); Core M1D-2407 (Nagashima et al., 2007); ODP site 1208 (Gylesjö, 2005).

the aridity through the history of aeolian flux is difficult. Nevertheless, the rapidly increasing flux of Asian dust matches the gradual cooling trend of global climate as reflected by the oxygen isotope of benthic foraminifera since 15 Ma (Zachos et al., 2001). The mountain building of Tibetan Plateau (Molnar and Stock, 2009; Royden et al., 2008; Xiao et al., 2012; Xu et al., 2013) may have play a primary role in driving the development of aridity of Asian interior between 25 and 15 Ma when the climate was consistently warm.

In addition to Pacific sediments, the loess deposits on the Chinese Loess Plateau (CLP) provided an unprecedented record of aridity history and variability in Asian interior since at least the late Oligocene (Guo et al., 2002; Qiang et al., 2011). The sedimentation rate of aeolian dust on CLP, however, exhibits a different evolution history. Differing from the records at site 1208, the sedimentation rates of Qin'an section on the CLP keeps relatively low from early Miocene to ~4 Ma (Guo et al., 2002) (Fig. 2). We suggest that the discrepancies may be attributed to the different atmospheric circulations patterns and dust sources for the Pacific sediments and Chinese loess deposits. It was reported that Pacific sediments were mainly derived from the Taklimakan desert by westerly wind, with long-distance transportation (Shao and Dong, 2006; Sun et al., 2001). The CLP basically received the dust from the proximal desert(s) via the near-surface winter monsoon (Che and Li, 2013; Chen and Li, 2011; Chen et al., 2007; Li et al., 2009).

5. Conclusion

The expanded sedimentation and the well-constrained age model of the ODP 1208 core provide a rare opportunity to explore the flux of Asian dust in North Pacific Ocean. Progressive increasing flux of the ODED has been recorded since 25 Ma. Evidences from trace element and radiogenic Nd and Sr isotopes suggest that the increasing ODED flux is caused by increasing flux of Asian dust rather than the increasing contribution from volcanic ash and authigenic mineral. The increasing flux of Asian dust since 25 Ma reflect a progressive aridification of Asian interior that might be linked to global cooling or regional mountain building.

Acknowledgements

This research used samples provided by the Ocean Drilling Program (ODP). ODP is sponsored by the U.S. National Science Foundation (NSF) and participating countries under the management of Joint Oceanographic Institutions, Inc. We thank Dr. James Gleason for providing samples of core LL44-GPC3. Zhimin Jiao, Tao Li, Zhong Chen, Fei Liu and Le Li are thanked for assistance in laboratory. We sincerely appreciate the constructive comments and suggestions from anonymous reviewers that have greatly improved this manuscript. This work was supported by National Natural Science Foundation of China (NSFC) (grant Nos. 41321062, 41230526, and 41422205). W. Z was also supported by the program B for outstanding PhD candidate of Nanjing University.

Appendix A. Supplementary data

Supplementary data associated with this article can be found, in the online version, at http://dx.doi.org/10.1016/j.aeolia.2016.09.004. These data include Google maps of the most important areas described in this article.

References

Aciego, S.M., Bourdon, B., Lupker, M., Rickli, J., 2009. A new procedure for separating and measuring radiogenic isotopes (U, Th, Pa, Ra, Sr, Nd, Hf) in ice cores. Chem. Geol. 266, 194–204.

An, Z., Kutzbach, J.E., Prell, W.L., Porter, S.C., 2001. Evolution of Asian monsoons and phased uplift of the Himalayan Tibetan plateau since Late Miocene times. Nature 411, 62–66.

Bailey, J.C., 1993. Geochemical history of sediments in the northwestern Pacific Ocean. Geochem. J. 2, 71–90.

Biscaye, P.E., Grousset, F.E., Revel, M., Van der Gaast, S., Zielinski, G.A., Vaars, A., Kukla, G., 1997. Asian provenance of glacial dust (stage 2) in the Greenland Ice Sheet Project 2 Ice Core, Summit. Greenland J. Geophys. Res. Oceans 102, 26765–26781.

Bory, A.J.M., Biscaye, P.E., Grousset, F.E., 2003. Two distinct seasonal Asian source regions for mineral dust deposited in Greenland (NorthGRIP). Geophys. Res. Lett. 30, 1167.

Cande, S.C., Kent, D.V., 1995. Revised calibration of the geomagnetic polarity timescale for the Late Cretaceous and Cenozoic. J. Geophys. Res. 100, 6093.

Che, X., Li, G., 2013. Binary sources of loess on the Chinese Loess Plateau revealed by U-Pb ages of zircon. Quat. Res. 80, 545–551.

Chen, J., Li, G.J., 2011. Geochemical studies on the source region of Asian dust. Sci. China Earth Sci. 54, 1279–1301.

Chen, Z., Li, G., 2013. Evolving sources of eolian detritus on the Chinese Loess Plateau since early Miocene: Tectonic and climatic controls. Earth Planet. Sci. Lett. 371–372, 220–225.

Chen, J., Li, G.J., Yang, J.D., Rao, W.B., Lu, H.Y., Balsam, W., Sun, Y.B., Ji, J.F., 2007. Nd and Sr isotopic characteristics of Chinese deserts: Implications for the provenances of Asian dust. Geochim. Cosmochim. Acta 71, 3904–3914.

Defant, M.J., Maury, R., Joron, J.-L., Feigenson, M.D., Leterrier, J., Bellon, H., Jacques, D., Richard, M., 1990. The geochemistry and tectonic setting of the northern section of the Luzon arc (The Philippines and Taiwan). Tectonophysics 183, 187–205.

Dubinin, A.V., Strekopytov, S., 2001. Behavior of rare earth elements during leaching of the oceanic sediments. Geoche. Int. 39, 692–701.

Dupont-Nivet, G., Krijgsman, W., Langereis, C.G., Abels, H.A., Dai, S., Fang, X., 2007. Tibetan plateau aridification linked to global cooling at the Eocene-Oligocene transition. Nature 445, 635–638.

Engelbrecht, J.P., Derbyshire, E., 2010. Airborne mineral dust. Elements 6, 241–246.

Ferrat, M., Weiss, D.J., Strekopytov, S., Dong, S.F., Chen, H.Y., Najorka, J., Sun, Y.B., Gupta, S., Tada, R., Sinha, R., 2011. Improved provenance tracing of Asian dust sources using rare earth elements and selected trace elements for palaeomonsoon studies on the eastern Tibetan Plateau. Geochim. Cosmochim. Acta 75, 6374–6399.

Guo, Z.T., Ruddiman, W.F., Hao, Q.Z., Wu, H.B., Qiao, Y.S., Zhu, R.X., Peng, S.Z., Wei, J. J., Yuan, B.Y., Liu, T.S., 2002. Onset of Asian desertification by 22 Myr ago inferred from loess deposits in China. Nature 416, 159–163.

Guo, Z.T., Peng, S.Z., Hao, Q.Z., Biscaye, P.E., An, Z.S., Liu, T.S., 2004. Late Miocene-Pliocene development of Asian aridification as recorded in the Red-Earth Formation in northern China. Glob. Planet. Change 41, 135–145.

Gylesjö, S., 2005. Data report: Late pleistocene terrigenous input to shatsky rise, site 1208. In: Bralower, T.J., Premoli Silva, I., Malone, M.J. (Eds.), Proceedings of the Ocean Drilling Program. Sci. Results, 198, pp. 1–7.

Hovan, S.A., Rea, D.K., Pisias, N.G., 1991. Late pleistocene continental climate and oceanic variability recorded in northwest Pacific sediments. Paleoceanography 6, 349–370.

Hyeong, K., Park, S.H., Yoo, C.M., Kim, K.H., 2005. Mineralogical and geochemical compositions of the eolian dust from the northeast equatorial Pacific and their implications on paleolocation of the Intertropical Convergence Zone. Paleoceanography 20, PA1010.

Jacobsen, S.B., Wasserburg, G.J., 1980. Sm-Nd isotopic evolution of chondrites. Earth Planet. Sci. Lett. 50, 139–155.

Janecek, T.R., 1985. Eolian sedimentation in the Northwest Pacific-Ocean – a preliminary examination of the data from deep-sea drilling project site 576 and site 578. In: Proceedings of the Ocean Drilling Program. Initial. Rep. 86, 589–603.

Janecek, T.R., Rea, D.K., 1983. Eolian deposition in the Northeast Pacific-Ocean – Cenozoic history of atmospheric circulation. Geol. Soc. Am. Bull. 94, 730–738.

Janecek, T.R., Rea, D.K., 1985. Quaternary fluctuations in the Northern Hemisphere trade winds and westerlies. Quat. Res. 24, 150–163.

Jiang, F., Frank, M., Li, T., Chen, T., Xu, Z., Li, A., 2013. Asian dust input in the western Philippine Sea: Evidence from radiogenic Sr and Nd isotopes. Geochem. Geophys. Geosystem. 14, 1538–1551.

Kawahata, H., Okamoto, T., Matsumoto, E., Ujiie, H., 2000. Fluctuations of eolian flux and ocean productivity in the mid-latitude north Pacific during the last 200 kyr. Qua. Sci. Rev. 19, 1279–1291.

Kepezhinskas, P., Mcdermott, F., Defant, M.J., Hochstaedter, A., Drummond, M.S., Hawkesworth, C.J., Koloskov, A., Maury, R.C., Bellon, H., 1997. Trace element and SrNdPb isotopic constraints on a three-component model of Kamchatka Arc petrogenesis. Geochim. Cosmochim. Acta 61, 577–600.

Leinen, M., Heath, G.R., 1981. Sedimentary indicators of atmospheric activity in the northern hemisphere during the Cenozoic. Palaeogeogr. Palaeoclimatol. Palaeoecol. 36, 1–21.

Li, G., Chen, J., Ji, J., Yang, J., Conway, T.M., 2009. Natural and anthropogenic sources of East Asian dust. Geology 37, 727–730.

Li, G., Pettke, T., Chen, J., 2011. Increasing Nd isotopic ratio of Asian dust indicates progressive uplift of the north Tibetan Plateau since the middle Miocene. Geology 39, 199–202.

McCulloch, M.T., Perfit, M.R., 1981. 143Nd/144Nd,87Sr/86Sr and trace element constraints on the petrogenesis of Aleutian island arc magmas. Earth Planet. Sci. Lett. 56, 167–179.

Miao, Y., Fang, X., Song, C., Yan, X., Zhang, P., Meng, Q., Li, F., Wu, F., Yang, S., Kang, S., 2016. Late Cenozoic fire enhancement response to aridification in mid-latitude Asia: Evidence from microcharcoal records. Qua. Sci. Rev. 139, 53–66.
Molnar, P., Stock, J.M., 2009. Slowing of India's convergence with Eurasia since 20 Ma and its implications for Tibetan mantle dynamics. Tectonics 28, TC3001.
Molnar, P., Tapponnier, P., 1975. Cenozoic tectonics of Asia: Effects of a continental collision: features of recent continental tectonics in Asia can be interpreted as results of the India-Eurasia collision. Science 189, 419–426.
Nagashima, K., Tada, R., Matsui, H., Irino, T., Tani, A., Toyoda, S., 2007. Orbital- and millennial-scale variations in Asian dust transport path to the Japan Sea. Palaeogeogr. Palaeoclimatol. Palaeoecol. 247, 144–161.
Nakai, S., Halliday, A.N., Rea, D.K., 1993. Provenance of dust in the Pacific Ocean. Earth Planet. Sci. Lett. 119, 143–157.
Olivarez, A.M., Owen, R.M., Rea, D.K., 1991. Geochemistry of eolian dust in Pacific pelagic sediments – Implications for paleoclimatic interpretations. Geochim. Cosmochim. Acta 55, 2147–2158.
Pettke, T., Halliday, A.N., Hall, C.M., Rea, D.K., 2000. Dust production and deposition in Asia and the North Pacific Ocean over the past 12 Myr. Earth Planet. Sci. Lett. 178, 397–413.
Pettke, T., Halliday, A.N., Rea, D.K., 2002. Cenozoic evolution of Asian climate and sources of Pacific seawater Pb and Nd derived from eolian dust of sediment core LL44-GPC3. Paleoceanography 17, 1031. 1010.1029/2001PA000673.
Piepgras, D.J., Jacobsen, S.B., 1992. The behavior of rare-earth elements in seawater – Precise determination of variations in the north Pacific water column. Geochim. Cosmochim. Acta 56, 1851–1862.
Piper, D.Z., Wandless, G.A., 1992. Hydroxylamine hydrochloride-acetic acid-soluble and insoluble fractions of pelagic sediment: readsorption revisited. Environ. Sci. Technol. 26, 2489–2493.
Pisias, N.G., Murray, R.W., Scudder, R.P., 2013. Multivariate statistical analysis and partitioning of sedimentary geochemical data sets: General principles and specific MATLAB scripts. Geochem. Geophys. Geosystem. 14, 1–6.
Qiang, X., An, Z., Song, YouGui, Chang, H., Sun, YouBin, Liu, WeiGuo, Ao, Hong, Dong, JiBao, Fu, ChaoFeng, Wu, Feng, Lu, FengYan, Cai, YanJun, Zhou, WeiJian, Cao, JunJi, XinWen, Xu, Ai, Li, 2011. New eolian red clay sequence on the western Chinese Loess Plateau linked to onset of Asian desertification about 25 Ma ago. Sci. China Earth Sci. 54, 136–144.
Raymo, M.E., Ruddiman, W.F., 1992. Tectonic forcing of late Cenozoic climate. Nature 359, 117–122.
Rea, D., Janecek, T., 1981. Mass-accumulation rates of the non-authigenic inorganic crystalline (eolian) component of deep-sea sediments from the western Mid-Pacific Mountains, Deep Sea Drilling Project Site 463. Init. Rep. 62, 653–659.
Rea, D.K., Janecek, T.R., 1982. Late Cenozoic changes in atmospheric circulation deduced from north Pacific eolian sediments. Mar. Geol. 49, 149–167.
Rea, D.K., Leinen, M., 1988. Asian aridity and the zonal westerlies – Late pleistocene and holocene record of eolian deposition in the Northwest Pacific-Ocean. Palaeogeogr. Palaeoclimatol. Palaeoecol. 66, 1–8.
Rea, D.K., Basov, I.A., Janecek, T.R., Palmer-Julson, A., 1993. Proceedings of the Ocean Drilling Program. Init. Rep. 145.
Rea, D.K., Snoeckx, H., Joseph, L.H., 1998. Late Cenozoic eolian deposition in the North Pacific: Asian drying, Tibetan uplift, and cooling of the northern hemisphere. Paleoceanography 13, 215–224.
Royden, L.H., Burchfiel, B.C., van der Hilst, R.D., 2008. The geological evolution of the Tibetan Plateau. Science 321, 1054–1058.
Seo, I., Lee, Y.I., Yoo, C.M., Kim, H.J., Hyeong, K., 2014. Sr-Nd isotope composition and clay mineral assemblages in eolian dust from the central Philippine Sea over the last 600 kyr: Implications for the transport mechanism of Asian dust. J. Geophys. Res. Atmos. 119. 2014JD022025.
Serno, S., Winckler, G., Anderson, R.F., Hayes, C.T., McGee, D., Machalett, B., Ren, H., Straub, S.M., Gersonde, R., Haug, G.H., 2014. Eolian dust input to the Subarctic North Pacific. Earth Planet. Sci. Lett. 387, 252–263.
Severmann, S., Mills, R.A., Palmer, M.R., Fallick, A.E., 2004. The origin of clay minerals in active and relict hydrothermal deposits. Geochim. Cosmochim. Acta 68, 73–88.
Shao, Y., Dong, C.H., 2006. A review on East Asian dust storm climate, modelling and monitoring. Glob. Planet. Change 52, 1–22.
Shipboard Scientific Party, 2002. Site 1208. In: Bralower, T.J., Premoli, S.I., Malone, M.J. (Eds.), Proceedings of the Ocean Drilling Program. Init. Rep. Ocean Drilling Program, pp. 1–93. College Station, TX.
Sholkovitz, E.R., 1989. Artifacts associated with the chemical leaching of sediments for rare-earth elements. Chem. Geol. 77, 47–51.
Snoeckx, H., Rea, D.K., Jones, C.E., Ingram, B.L., 1992. 14. Eolian and silica deposition in the central north pacific: results from sites 885/886. In: Proceedings of the Ocean Drilling Program. Init. Rep. 145.
Stancin, A.M., Gleason, J.D., Rea, D.K., Owen, R.M., Moore Jr., T.C., Blum, J.D., Hovan, S. A., 2006. Radiogenic isotopic mapping of late Cenozoic eolian and hemipelagic sediment distribution in the east-central Pacific. Earth Planet. Sci. Lett. 248, 840–850.
Sun, Y.B., An, Z.S., 2002. History and variability of Asian interior aridity recorded by eolian flux in the Chinese Loess Plateau during the past 7 Ma. Sci. China, Ser. D Earth Sci. 45, 420–429.
Sun, Y., An, Z., 2005. Late Pliocene-Pleistocene changes in mass accumulation rates of eolian deposits on the central Chinese Loess Plateau. J. Geophys. Res. 110, D23101. 23110.21029/22005JD006064.
Sun, J.M., Zhang, M.Y., Liu, T.S., 2001. Spatial and temporal characteristics of dust storms in China and its surrounding regions, 1960–1999: Relations to source area and climate. J. Geophys. Res. Atmos. 106, 10325–10333.
Svensson, A., Biscaye, P.E., Grousset, F.E., 2000. Characterization of late glacial continental dust in the Greenland Ice Core Project ice core. J. Geophys. Res. Atmos. 105, 4637–4656.
Tapponnier, P., Xu, Z.Q., Roger, F., Meyer, B., Arnaud, N., Wittlinger, G., Yang, J.S., 2001. Oblique stepwise rise and growth of the Tibet plateau. Science 294, 1671–1677.
Taylor, S.R., McLennan, S.M., 1985. The Continental Crust: Its Composition and Evolution. Blackwell, Oxford.
Venti, N.L., Billups, K., 2012. Stable-isotope stratigraphy of the Pliocene-Pleistocene climate transition in the northwestern subtropical Pacific. Palaeogeogr. Palaeoclimatol. Palaeoecol. 326–328, 54–65.
Wang, G.C., Cao, K., Zhang, K.X., Wang, A., Liu, C., Meng, Y.N., Xu, Y.D., 2011. Spatio-temporal framework of tectonic uplift stages of the Tibetan Plateau in Cenozoic. Sci. China Earth Sci. 54, 29–44.
Wang, E., Kirby, E., Furlong, K.P., van Soest, M., Xu, G., Shi, X., Kamp, P.J.J., Hodges, K. V., 2012. Two-phase growth of high topography in eastern Tibet during the Cenozoic. Nat. Geosci. 5, 640–645.
Weber, E.T., Owen, R.M., Dickens, G.R., Halliday, A.N., Jones, C.E., Rea, D.K., 1996. Quantitative resolution of eolian continental crustal material and volcanic detritus in North Pacific surface sediment. Paleoceanography 11, 115–127.
Woodhead, J.D., 1989. Geochemistry of the Mariana arc (western Pacific): Source composition and processes. Chem. Geol. 76, 1–24.
Xiao, G.Q., Guo, Z.T., Dupont-Nivet, G., Lu, H.Y., Wu, N.Q., Ge, J.Y., Hao, Q.Z., Peng, S. Z., Li, F.J., Abels, H.A., Zhang, K.X., 2012. Evidence for northeastern Tibetan Plateau uplift between 25 and 20 Ma in the sedimentary archive of the Xining Basin. Northwestern China. Earth Planet. Sci. Lett. 317, 185–195.
Xu, Z., Wang, Q., Pêcher, A., Liang, F., Qi, X., Cai, Z., Li, H., Zeng, L., Cao, H., 2013. Orogen-parallel ductile extension and extrusion of the Greater Himalaya in the late Oligocene and Miocene. Tectonics 32, 191–215.
Xu, Z., Li, T., Clift, P.D., Lim, D., Wan, S., Chen, H., Tang, Z., Jiang, F., Xiong, Z., 2015. Quantitative estimates of Asian dust input to the western Philippine Sea in the mid-late Quaternary and its potential significance for paleoenvironment. Geochem. Geophys. Geosystem. 16, 3182–3196.
Yin, A., 2010. Cenozoic tectonic evolution of Asia: A preliminary synthesis. Tectonophysics 488, 293–325.
Zachos, J., Pagani, M., Sloan, L., Thomas, E., Billups, K., 2001. Trends, rhythms, and aberrations in global climate 65 Ma to present. Science 292, 686–693.
Zhang, W., Chen, J., Li, G., 2015. Shifting material source of Chinese loess since reflected by Sr isotopic composition. Sci. Rep. 5, 10235.
Zhao, W., Sun, Y., Balsam, W., Lu, H., Liu, L., Chen, J., Ji, J., 2014. Hf-Nd isotopic variability in mineral dust from Chinese and Mongolian deserts: implications for sources and dispersal. Sci. Rep. 4, 5837.
Zhao, W., Sun, Y., Balsam, W., Zeng, L., Lu, H., Otgonbayar, K., Ji, J., 2015. Clay-sized Hf-Nd-Sr isotopic composition of Mongolian dust as a fingerprint for regional to hemispherical transport. Geophys. Res. Lett. 42, 5661–5669.
Zheng, H., Powell, C.M., Rea, D.K., Wang, J., Wang, P., 2004. Late Miocene and mid-Pliocene enhancement of the East Asian monsoon as viewed from the land and sea. Glob. Planet. Change 41, 147–155.
Ziegler, C.L., Murray, R.W., 2007. Geochemical evolution of the central Pacific Ocean over the past 56 Myr. Paleoceanography 22, PA2203.
Ziegler, C.L., Murray, R.W., Hovan, S.A., Rea, D.K., 2007. Resolving eolian, volcanogenic, and authigenic components in pelagic sediment from the Pacific Ocean. Earth Planet. Sci. Lett. 254, 416–432.